the low-temperature forms of the homopolymer. It is possible that this corresponds to some sort of liquid crystalline structure. However, the structure is not nematic: the first layer line reflection is definite evidence for a specific or preferred axial register of adjacent chains.

The observed data for the copolymers could be explained by segregation of homopoly(*p*-hydroxybenzoate) sequences, as might be expected if there is extensive blockiness. This explanation of electron diffraction data for the copolymers has been given in a recent paper by Zachariades et al.[19] However, if this is the case it is surprising that the ordered structures have the high-temperature form of the homopolymer. It seems more likely that the ordered regions contain sequences *rich* in *p*-hydroxybenzoate, in which some ethylene terephthalate units are present as defects. Such defects could probably be tolerated in the open high-temperature form of the homopolymer but could prevent adoption of the more compact low-temperature crystalline structure. The ordered structures are only a fraction of the total fiber, and the disordered regions responsible for the diffuse equatorial sections probably contain higher proportions of ethylene terephthalate. This view is supported by the thermal analyses of Meesiri et al.,[12] which demonstrate the existence of two phases in the copolymers. The melting behavior of the higher melting phase, which is probably the ordered region seen here, suggests that this consists of segregated copolymer rich in *p*-hydroxybenzoate rather than homopolymer blocks. For the 80% copolymer, even a fully random structure will contain extensive sequences rich in *p*-hydroxybenzoate, and thus it is not surprising that this composition is more ordered than the 60% copolymer.

Acknowledgment. This work has been supported by grants from the Deutsche Forschungsgemeinschaft and from the United States National Science Foundation (DMR78-24150 and DMR81-07130). A visiting professorship to John Blackwell from the Deutsche Forschungsgemeinschaft is gratefully acknowledged.

References and Notes

(1) Jin, J. I.; Antoun, S.; Ober, C.; Lenz, R. W. *Br. Polym. J.* **1980**, *12*, 132–146.
(2) Calundann, G. W.; Davis, H. C.; Gorman, Z. J.; Mininni, R. M. *U.S. Pat.* 4 083 829, 1978 (Celanese).
(3) Calundann, G. W. *U.S. Pat.* 4 067 852, 1978; 4 130 545, 1978, (Celanese).
(4) Kuhfuss, H. F.; Jackson, W. T. *U.S. Pat.* 3 804 805, 1974 (Tennessee Eastman).
(5) Jackson, W. J.; Kuhfuss, H. F. *J. Polym. Sci., Polym. Chem. Ed.* **1976**, *14*, 2043–2058.
(6) Cottis, S. G.; Economy, J.; Nowak, B. E. *U.S. Pat.* 3 637 595, 1972 (Carborundum).
(7) Schaefgen, J. R. *U.S. Pat.* 4 118 372, 1978 (du Pont).
(8) Goodman, I.; McIntyre, J. E.; Stimpson, J. W. *U.S. Pat.* 3 321 437, 1967 (I.C.I.).
(9) Economy, J.; Storm, R. S.; Markovich, V. I.; Cottis, G. G.; Nowak, B. E. *J. Polym. Sci., Polym. Chem. Ed.* **1979**, *14*, 2207–2224.
(10) Lenz, R. W.; Feichtinger, K. A. *Polym. Prepr., Am. Chem. Soc., Div. Polym. Chem.* **1979**, *20*, 114–117.
(11) Menczel, J.; Wunderlich, B. *J. Polym. Sci., Polym. Phys. Ed.* **1980**, *18*, 1433–1438.
(12) Meesiri, W.; Menczel, J.; Gaur, U.; Wunderlich, B. *J. Polym. Sci., Polym. Phys. Ed.* **1982**, *20*, 719–728.
(13) Hay, I. Abstracts of the 39th Pittsburgh Diffraction Conference, Cleveland, Ohio, Nov 1981.
(14) Blackwell, J.; Gutierrez, G. A. *Polymer* **1982**, *23*, 671–675.
(15) Schwarz, G.; Kricheldorf, H. R., submitted to *Makromol. Chem.*
(16) Lieser, G., submitted to *J. Polym. Sci., Polym. Phys. Ed.*
(17) Tadokoro, H. In "Structure of Crystallin Polymers"; Wiley: New York, 1979; p 398.
(18) Hummel, J. P.; Flory, P. J. *Macromolecules* **1980**, *13*, 479–484.
(19) Zachariades, A. E.; Economy, J.; Logan, J. A. *J. Appl. Polym. Sci.* **1982**, *27*, 2009–2014.

Structure and Degradation of an Intractable Polymeric System: Melamine Formaldehyde Cross-Linked Acrylic Coatings†

A. D. English* and D. B. Chase

Central Research and Development Department, Experimental Station, E. I. du Pont de Nemours and Company, Wilmington, Delaware 19898

H. J. Spinelli

Finishes and Fabricated Products Department, Experimental Station, E. I. du Pont de Nemours and Company, Wilmington, Delaware 19898.
Received October 27, 1982

ABSTRACT: Curing and degradation chemistry at the primary cross-linking site in pigmented melamine formaldehyde cross-linked acrylic copolymer coatings have been characterized as a function of depth by using the complementary techniques of diffuse reflectance infrared spectroscopy and solid-state ^{13}C NMR. The curing of an acid-catalyzed coating is shown to go to completion under the conditions used with no significant concurrent melamine self-condensation reactions. Degradation is promoted by the presence of heat and/or light, residual acid, and atmospheric water; the degradative pathway invokes irreversible acid-catalyzed hydrolysis of (i) unreacted melamine methoxymethyl moieties throughout the coating and (ii) primary cross-links only at the very surface.

Introduction

The cross-linking and degradation chemistry of melamine formaldehyde–acrylic copolymer coatings have been a field of renewed interest recently.[1–4] One aspect of these coatings that makes them difficult to study is the intractability of the system to conventional physical techniques. In the cured state the system consists of a highly cross-linked polymeric network in which a large amount of finely dispersed pigment, metallic flake, and other additives are present. The system is not amenable to conventional transmission infrared spectroscopic studies due to the high scattering power of the additives. Also, solution NMR techniques are not of use since the act of dissolution greatly perturbs, if not destroys, the primary melamine–acrylic cross-linking sites. An additional complication with this system is often the poorly defined nature of the melamine formaldehyde cross-linking agent and the acrylic

† Contribution No. 3086.

0024-9297/83/2216-1422$01.50/0

copolymer. A final complication regarding the degradation chemistry is that previous studies have concentrated on the use of artificial laboratory weathering devices, which are known to not always reliably simulate natural conditions.

We have used diffuse reflectance infrared spectroscopy and solid-state ^{13}C NMR techniques to study the cross-linking and degradation chemistry of a melamine formaldehyde cured acrylic copolymer coating. The melamine cross-linking agent has been characterized by NMR and IR methods. The bulk composition of the cured unweathered film has been semiquantitatively analyzed by solid-state ^{13}C NMR, and a depth profile of weathering chemistry has been obtained by using diffuse reflectance infrared spectroscopy. These data allow us to identify the extent of cross-linking, to establish the molecular composition after curing, and to obtain mechanistic insight into degradation chemistry taking place under realistic exposure conditions. The insight obtained has implications as to methods of inhibiting degradation.

Experimental Section

Coating Preparation. The acrylic resin, a copolymer of methyl methacrylate/butyl acrylate/hydroxyethyl acrylate, was prepared by standard solution polymerization techniques. The initiator was 2,2′-azobis(isobutyrontrile) and the chain-transfer agent was 2-mercaptoethanol.

Coatings were prepared by mixing the acrylic resin with Resimene X-747 (nominally hexakis(methoxymethyl)melamine) at a 70.4/29.6 weight ratio in methyl ethyl ketone and adding 0.30% *p*-toluenesulfonic acid (PTSA) as a catalyst. The pigmentation in the coating was as follows: aluminum flake (0.8% of binder), titanium dioxide (0.1%), carbon black (0.4%), phthalocyanine blue (1.0%), fumed silica (1.5%), and Monastrol Red (0.2%). The coatings were sprayed on zinc phosphated steel panels primed with a standard alkyd primer. The films were baked for 30 min at 120 °C. The cured film thicknesses were 50 ± 5 μm, as measured by a Permascope thickness gauge (ASTM D-1400, procedure C). Film hardnesses were approximately 12.7 knoops, as measured by a Tukon knoop hardness tester (ASTM D-1474). Specular gloss readings were obtained on a standard gloss meter (ASTM 523, method D).

Panels were exposed in Florida on a black box rack for a total of 24 months. The panels faced south and were inclined at an elevation of 5° above horizontal. After exposure, the panels were washed with a mild soap solution, rinsed, and dried before being analyzed.

Coating Depth Profiling. Depth profiling of coatings that had been applied to steel panels was accomplished by abrading the panel with 600-A Tufbak Durite T44 cloth (14-μm silicon carbide particle size) in a water medium. After a short period of abrasion (ca. 30 s), the material removed was collected, filtered, and dried in a vacuum oven at 55–65 °C for 24–48 h to remove residual water. This procedure was repeated 10–30 times on each panel until the primer was barely visible. The material collected in each sample was then cryogenically milled and dried in a vacuum oven at 55–65 °C for 24–48 h. This procedure produces particle sizes prior to cryomilling of ≈1 μm, which then agglomerate upon drying. The cryomilling procedure is necessary to produce infrared spectra that are particle-size independent (see below). The distribution of material collected in each sample was estimated, from results on multicoat systems, to contain approximately 70% from the region claimed to be sampled and approximately 30% from other sections. Therefore, the depth profiling analysis is smoothed by the imprecision in cross-section depth. Cross-section depths are calculated on a fractional weight basis.

Reference Materials. A second acrylic resin was prepared by similar polymerization methods from methyl methacrylate, butyl acrylate, styrene, and hydroxyethyl acrylate (MMA/BA/S/HEA). This resin was cast with Resimene X-747 in a 70.0/30.0 weight ratio with 0.2 wt % PTSA in methyl ethyl ketone and subsequently cured at 120 °C for 30 min. This clear coating was used in the initial infrared and NMR curing studies.

2-Chloro-4,6-bis(propylamino)-*s*-triazine (CBT) was synthesized as a stable reference compound for infrared determination of NH content. CBT was synthesized from *n*-propylamine and cyanuric chloride. Cyanuric chloride (0.3 mol) was slowly added with caution over a period of 4 h to 1.5 mol of *n*-propylamine in 150 mL of tetrahydrofuran in a three-neck flask equipped with a stirrer and thermometer that was thermostated with an ice bath to 0–20 °C. After 1 h of stirring at room temperature, the slurry was heated to 50 °C for 16 h with stirring. The slurry was neutralized with concentrated NaOH solution and stirred for 1 h. The slurry was then evaporated on a rotoevaporator, and the collected solids were washed with water three times. The resulting wet solids were dissolved in methylene chloride, and the aqueous layer was discarded. The methylene chloride solution was evaporated on a rotoevaporator, and the resulting material was recrystallized from hot dimethyl sulfoxide and confirmed to be CBT (mp 208–210 °C) by ^1H and ^{13}C NMR and elemental analysis. (Anal. Calcd: C, 47.05; H, 6.97; N, 30.5, Cl, 15.5. Found: C, 47.07; H, 7.01; N, 30.35; Cl, 15.24).

Resimene X-747 (Monsanto) was used without further purification as a reference standard for $>NCH_2OCH_3$ in the infrared analysis. ^1H and ^{13}C NMR confirmed that the melamine in this product is essentially hexakis(methoxymethyl)melamine with a small fraction (<5%) of the amine substituents being >NH or $>NCH_2OH$. Infrared analysis (see below) indicated that ~3% of the amine substituents were either >NH or $>NCH_2OH$.

Infrared Spectroscopy. All infrared spectra were obtained with a Nicolet 7199 FT-IR spectrometer operating in a diffuse reflectance configuration. The design of the diffuse reflectance bench was similar to that of Fuller and Griffiths.[5] Two hundred fifty-six interferograms were averaged, apodized with a polynomial function F_3,[6] and transformed to give 2-cm^{-1}-resolution spectra. Finely powdered potassium bromide was used as a reflectance standard for the midrange infrared region and reflectance spectra were converted to Kubelka–Munk units before the spectral bands of interest were integrated. It is known that diffuse reflectance spectra can exhibit a particle size dependency, which could affect both bandwidth and peak intensity. One of the samples, prepared as discussed above, was chosen at random and run through a Sonic-Sifter to characterize the particle size distribution. Ninety percent of the sample passed through a 44-μm mesh. Previous work has shown that once the particle size is reduced below 30 μm, no further particle size dependence is observed. Furthermore, the spectrum obtained with the seived material was identical with the spectrum of the unseived sample.

NMR Spectra. NMR spectra were recorded on a Bruker CXP300 NMR spectrometer. Solid-state ^{13}C NMR spectra were obtained with cross polarization, dipolar decoupling, and spin-temperature alternation techniques,[7] using a radio-frequency field strength γH_1 = 64 kHz with a cross polarization time of 5 ms to minimize intensity distortion in spin counting due to varying strength of carbon–proton dipolar interactions among individual carbon nuclei. Samples were contained in rotors of the Beams[8]–Andrew[9] geometry fabricated from perdeuterated poly(methyl methacrylate). Sample spinning speeds were chosen to minimize spinning sideband overlap and a 5.0-kHz spinning rate appeared to be optimium at this field strength and rotor size.

Results

Recent investigations into the curing chemistry of intractable polymer systems have demonstrated that solid-state ^{13}C NMR spectra may be used to examine curing chemistry in thermally polymerized polyimides[10] and expressed hope[11] that these techniques may be used in conjunction with infrared spectroscopy to give further mechanistic insight. We have used both solid-state ^{13}C NMR and diffuse reflectance infrared spectroscopies to characterize the curing and degradation chemistry of melamine formaldehyde cross-linked acrylic copolymer coatings.

NMR Analysis. Solid-state ^{13}C NMR spectra are of particular use in characterizing the curing chemistry of this system because pigments and other fillers used in the formulation of these coatings are transparent so long as they are noncarbonaceous, are nonferromagnetic, and when

conductive, are sufficiently dilute to not significantly detune the radio-frequency tuned circuits. The basic techniques have been described in the Experimental Section and these have been supplemented by two recently developed methods to enable us to obtain reproducible semiquantitative compositional analyses. The resolution achievable in this experiment is governed by a large number of factors,[12] where one of the more serious losses of resolution may be caused by misadjustment of the magic angle. A common alignment procedure is to adjust the angle with a calibration sample containing a ^{13}C nucleus that possesses a large chemical shift anisotropy and then replacing the calibration sample with the sample of interest. This approach is not entirely satisfactory because the angle the spinning axis of the rotor makes with the static magnetic field is a weak function of both the manner in which the sample is packed and the specific rotor used and a strong function of the driving pressure (spinning rate). In these experiments, the polymeric samples contain carbon nuclei with large chemical shift anisotropic that cannot be completely spun out at a magnetic field strength of 7 T to yield only an isotropic resonance; therefore, the spinning rate must be varied in an attempt to disentangle isotropic lines from spinning sidebands. This requirement makes the usual procedure quite time-consuming and in practice inaccurate. We have employed the method of Frye and Maciel[13] to adjust the magic angle via observation of the rotational spin echos produced from the quadrupolar-broadened ^{79}Br signal of a small amount (~<10%) of KBr that has been mixed with the sample. The rotational spin-echo pattern in the frequency or time domain is sensitive to the magic angle adjustment and may be conveniently used to adjust the magic angle when the spinning gas pressure or temperature is changed without sample removal or spectrometer retuning.

Extraction of quantitative chemical compositions from cross polarization/magic angle spinning ^{13}C NMR spectra is complicated by spin polarization dynamics and the distribution of significant signal intensity into spinning sidebands for many of the magnetically distinct carbon nuclei at the magnetic field strength and spinning speeds we employ. The question of the relationship between spin polarization dynamics and spectral populations has been dealt with previously;[14-16] in this case where proton spin diffusion is able to produce a homogeneous spin bath that is characterized by a singly exponential $T_{1\rho}(H)$, we have used long cross polarization times (5 ms) and large spin-locking fields (γH_1 = 64 kHz) to obtain representative spectral populations even for those carbon nuclei with small static proton–carbon dipolar interaction. The question of extraction of quantitative spectral populations from spectra containing many spinning sidebands has been dealt with recently;[17,18] however, we are not yet equipped to implement this "phase-alternated spinning sideband" technique and have chosen to use the method of Herzfeld and Berger[19] to estimate spinning sideband intensity patterns and to use these estimates to correct the spectral populations extracted from the isotropic resources alone.

Figure 1 illustrates a ^{13}C solid-state NMR spectrum of an unpigmented melamine formaldehyde–acrylic copolymer coating prepared from MMA/BA/S/HEA and cross-linked with Resimene X-747 (see above). Chemical shifts and spectral assignments are given in Table I. This spectrum illustrates that all carbon nuclei, which are distinct on the most elementary level (not comparable to high-resolution solution NMR), may be assigned in the spectrum. In Table I we have also tabulated integrated intensities measured from this spectrum, which have been

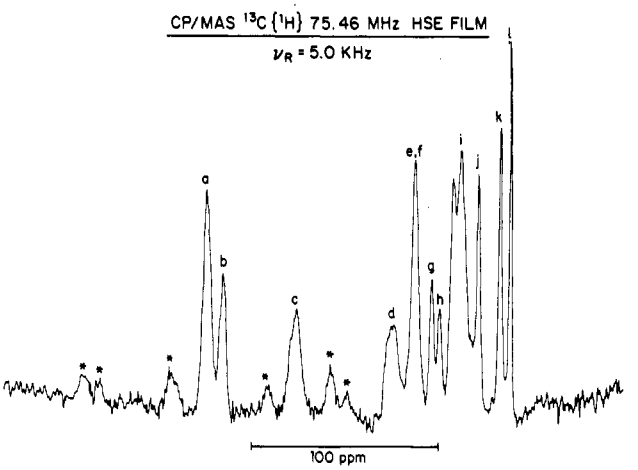

Figure 1. Solid-state ^{13}C spectrum of a melamine formaldehyde cross-linked acrylic copolymer coating. The static magnetic field is 7.0 T and the spinning rate is 5.0 kHz. Chemical shifts and assignments are given in Table I and features marked with an asterisk are resolved spinning sidebands.

Table I
Composition of MMA/BA/S/HEA Cross-Linked with Resimene X-747

structure	δ[a]	concentration, exptl	concentration, calcd
a, acrylic carboxyl	175.2	2.6	2.3
b, triazine ring	166.5	1.7	1.1
c, styrene aromatic	127.8	3.3	2.8
d, NCH_2O	76.6	1.5	2.1
e, f, OCH_2CH_2O + OCH_3 (NBA)	64.5	2.3	2.7
g, NCH_2OCH_3	55.5	0.8	1.3
h, OCH_3 (MMA)	51.6	0.6	0.5
i, acrylic backbone	44.4, 40.4	3.9	5.5
j, CH_2 (NBA)	31.1	1.1	1
k, α-CH_3 (MMA) + CH_2 (NBA)	19.3	1.1	1.5
l, CH_3 (NBA)	13.9	≡1	≡1

[a] δ in ppm from $(CH_3)_4Si$; referenced to glycine at δ = 176.1.

corrected for estimated spinning sideband contributions and additionally, intensities calculated from the known initial composition of the film assuming complete primary cross-linking and no side reactions (see below). The experimental and calculated results are in reasonable qualitative agreement and support the infrared spectroscopic results (see below) that the primary cross-linking goes to completion under the cure conditions used and the extent of competing side reactions is minimal. Failure of reaction 1 in Figure 3 to go to completion would appear as an increase in intensity of resonance g in Table I and significant self-condensation would appear as a further diminution of resonance d. We have also obtained solid-state ^{13}C NMR spectra of a few selected pigmented coatings, and these results are similar to those found for the unpigmented system. At this time the NMR results are of use to corroborate the infrared spectroscopic results; truly quantitative information will be obtained only with a quantitative calculation of spinning sideband intensities and spectral simulation.[20]

Infrared Analysis. Diffuse reflectance infrared spectroscopy has been used to characterize both the curing and degradation chemistry of melamine formaldehyde cross-linked acrylic copolymer coatings. This technique is useful for not only clear coats but most appropriately for coatings that contain pigment, aluminum flake, and other fillers that are by their very nature intended to be efficient

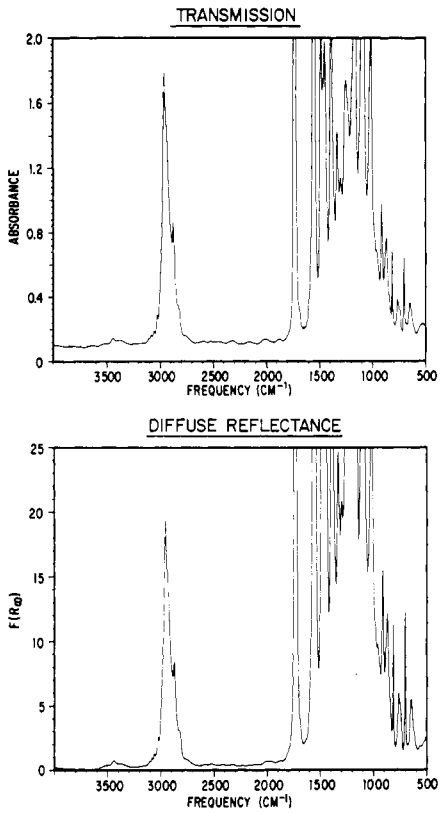

Figure 2. Transmission and diffuse reflectance infrared spectra of a clear melamine formaldehyde cross-linked acrylic copolymer coating.

scatterers and thus cannot usually be examined with transmission infrared techniques. Figure 2 illustrates both a conventional transmission and a diffuse reflectance infrared spectrum of a clear coating (MMA/BA/S/HEA and Resimene X-747). A comparison between the methods must be made by using a clear formulation because transmission infrared spectra of highly pigmented coatings are grossly distorted due to high scattering levels when spectra are collected at usual concentrations; at very dilute concentrations (to avoid intense scattering) the transmission spectra are heavily contaminated with adventitious contaminants. The infrared bands of interest may be integrated and the relative integrals of the bands in each spectrum are within ±3% of each other when peak absorbance values of less than 2.0 and peak Kubelka–Munk values less than 20 are used. The regions of the infrared spectrum of interest are 816 cm^{-1} (melamine triazine ring deformation), 913 and 870 cm^{-1} (methoxymethyl deformation), ~3570 cm^{-1} (ROH stretch), and ~3350 cm^{-1} (>NH stretch). In all cases, the ratio of the integrated intensity of the band of interest to the integrated intensity of the melamine triazine ring deformation has been used to measure normalized intensity. As reference compounds CBT and Resimene X-747 (see Experimental Section) have been used as primary standards for >NH and $>NCH_2OCH_3$, respectively.

Infrared analysis of both clear and pigmented films prepared as described in the Experimental Section shows complete consumption of all hydroxyl functionality on the acrylic copolymer within ±2% when cured at 120 °C for 30 min. Additionally, there is no detectable generation of free amine, and the loss of methoxymethyl functionality on the melamine is equivalent on a molar basis to consumption of hydroxyl on the acrylic copolymer within the accuracy (±5%) of the measurement of the methoxymethyl functionality. These observations are in agreement with previous work[2] that demethylation (reaction 2, Figure 3),

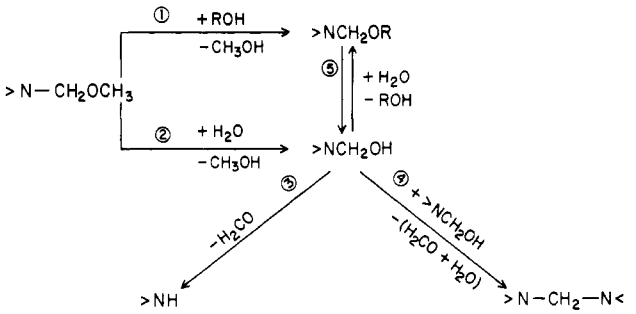

Figure 3. Elementary cross-linking and hydrolytic degradation reactions involved in melamine formaldehyde ($>NCH_2OCH_3$) cross-linking reactions with hydroxy-functionalized acrylic copolymers (ROH).

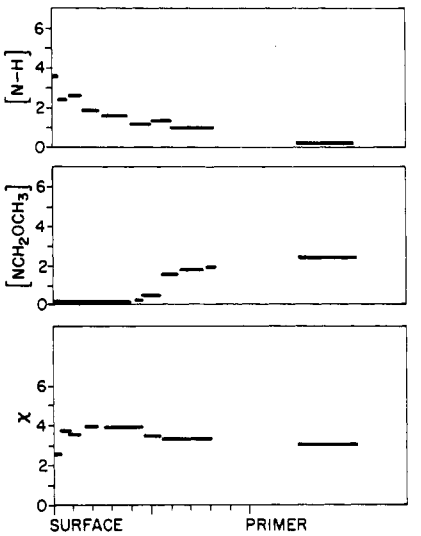

Figure 4. Depth profile of free amine, methoxymethyl, and primary cross-link density of a 50-μm-thick blue-pigmented melamine formaldehyde cross-linked acrylic copolymer coating that was exposed for 2 years in Florida. Bars on the right-hand side of the graph indicate concentrations expected in the absence of degradation.

deformylation (reaction 3), and melamine self-condensation (reaction 4) do not occur to a significant extent and that transetherification (reaction 1) goes essentially to completion under these curing conditions with a fully methylated melamine. Figure 3 outlines the most elementary scheme of melamine formaldehyde cross-linking and hydrolytic degradation reactions that must be considered. These results for the bulk curing of the coatings indicate that only reaction 1 is of significance during the curing step with the conditions we have used, and thus the initial chemical state of the coating to be exposed is known.

Pigmented coatings that had been exposed in Florida for 2 years were depth profiled, via the abrasion procedure described in the Experimental Section. Seventeen samples were collected and analyzed by diffuse reflectance infrared analysis for ROH, >NH, $>NCH_2OCH_3$, and melamine concentration as a function of depth. The melamine concentration varied less than ±10% in a nonsystematic manner as a function of depth in the coating and was therefore used as an internal standard. There was no alcohol functionality detectable in any of the samples. The remainder of the data obtained are shown in Figure 4 and illustrate the following: (i) >NH concentration is highest at the surface and decreases monotonically as the depth of the sample increases, approaching the value (right-hand side of graph) calculated from the starting material with the knowledge that only reaction 1 is significant and goes to completion; (ii) $>NCH_2OCH_3$ concentration is near zero

at the surface and becomes nonzero near the middle of the film and once again approaches the value (right-hand side of graph) calculated from the starting material and known reaction chemistry; (iii) X is essentially independent of depth and is very close to that calculated (right-hand side of graph) from the starting material and known reaction chemistry except at the surface where it is 30% smaller. X equals (6 - [>NH] - [$>NCH_2OCH_3$]) and is a measure of the sum of primary cross-links (reaction 1) and melamine self-condensation (reaction 4) (see Discussion). As noted, each graph in Figure 4 indicates the amount of each species that is expected to be present in the absence of weathering based upon our observations of the curing chemistry of each film. It is clear that there has been significant production of >NH and loss of $>NCH_2OCH_3$ and that X is invariant to weathering except at the surface to depth of ≈5–10 μm. This observation is not at variance with the traditional method of characterizing film degradation: gloss loss. The gloss of this coating decreased from 60 to 30 during the 2 years of Florida weathering.

Discussion

The structure and degradation chemistry of melamine formaldehyde cross-linked acrylic copolymer coatings that we have discussed are limited only to considerations of reactions at or near the primary cross-link site involving the melamine with the acrylic copolymer hydroxyl site or with another melamine. There exists copious evidence in the literature that physical appearance degradation occurs in pure acrylic coatings, and similar degradative pathways involving only acrylic backbone degradation are expected to exist in the system we have examined as well. Nevertheless, we have chosen to confine ourselves to an examination of the reactions and degradation chemistry at the primary cross-linking site because this is the major difference between the two systems.

Figure 3 illustrates that the number of species that must be identified and followed in the most simplistic examination of primary cross-linking chemistry followed is six ($>NCH_2OCH_3$, $>NCH_2OR$, $>NCH_2OH$, >NH, $>NCH_2N<$, melamine) if we wish to completely characterize even this elementary scheme. We can reduce this number with the following conditions: (i) Reaction 3 has been shown[1,2] to be facile in fully alkylated systems and we do not observe methylol groups in the infrared spectra. (ii) The relative concentrations of $>NCH_2OCH_3$, >NH, ROH, and melamine can be measured quantitatively by infrared methods. (iii) The consumption of ROH during cure is assumed to be accomplished by only reaction 1. With these conditions it is possible to measure >NH and $>NCH_2OCH_3$ relative to melamine concentration and also to calculate from mass balance a cross-link parameter (X) that is the sum of $>NCH_2OR$ and $>NCH_2N<$ (or other condensed species) relative to melamine. The calculated value (X) may then be compared to the expected concentration of NCH_2OR obtained from ROH consumption to evaluate the likelihood of any condensation products (reaction 4). An examination of Figure 4 shows that the value of X obtained throughout the coating except at the very surface is quite close to that calculated from ROH consumption. Additionally, we find no infrared spectroscopic evidence for the presence of $>NCH_2N<$[21] or free ROH at any point in the coating profile. These observations, when taken as a whole, lead to the following description of the primary cross-link reaction and degradation chemistry that takes place under the conditions used:

1. The primary cross-linking reaction (reaction 1) goes to completion and no other reaction takes place to a significant extent when the cure is 30 min at 120 °C.
2. Degradation under realistic exposure conditions is facilitated near the surface, with all degradation below the surface 2–5-μm layer in the coating that remains after exposure attributable to reactions 2 and 3. If catastrophic degradation occurs at the coating surface, this material would be lost from the panel and would not be observable with our methods. Measurement of film thickness is insufficiently accurate (±10%) to assess this possibility with precision; however, physical loss of film thickness appears to be small (<∼10%) for these coatings.
3. Primary cross-link degradation is observed only at the very surface, where X is decreased by ∼30%, and there is no evidence for either ROH or $>NCH_2OH$ in this layer.
4. There is no evidence for any significant amount of melamine–melamine self-condensation at any time during cure or exposure.

This description will lead us to speculate about the pathway of primary cross-link degradation in this system. The efficacy of reactions 2 and 3 leads us to postulate that residual acid remaining from the cure leads to acid-catalyzed hydrolysis of $>NCH_2OCH_3$ to produce >NH along with the volatile products of methanol and formaldehyde. This reaction is most enhanced near the surface, where it is more likely that photooxidation or some other process has caused sufficient degradation to increase the affinity of the initially hydrophobic coating to water and/or to increase the mobility of water and residual acid. It would seem reasonable that this same acid-catalyzed hydrolysis would promote reaction 5 and lead to loss of primary cross-links; however, reaction 5 produces nonvolatile products that may be able to react to re-form the cross-link before either product undergoes further reaction and thus make it appear that the primary cross-link is not susceptible to hydrolysis. Additionally, we have observed that these coatings are much more resistant to degradation in an environment that lacks either high humidity or high solar flux.[22] Thus it appears that a plausible pathway for degradation in this melamine formaldehyde cross-linked acrylic coating system is as follows:

1. The initially hydrophobic surface of the coating is oxidized either photolytically or thermally, which increases the concentration and/or mobility of water and increases the mobility of the residual acid.
2. Acid-catalyzed hydrolysis of $>NCH_2OCH_3$ to form free amine is favored due to production of volatile products that may escape to the atmosphere.
3. Acid-catalyzed hydrolysis of primary cross-links is reversible and therefore unobserved except where the hydrolysis products undergo further reaction to prevent back-reaction. At the very surface of the coating, where there is insufficient pigment to provide an effective solar screen, ROH and $>NCH_2OH$ in reaction 5 are consumed presumably by photooxidation and reaction 3, respectively.
4. Melamine self-condensation, reaction 4, does not occur to a significant extent.

The proposed pathway requires the presence of heat and/or light, residual acid, and atmospheric water to promote degradation. This implies that removal of any of these three components should retard degradation. This pathway also suggests that accelerated weathering studies that employ a much higher light flux for a shorter period of time may well give an unrepresentatively large amount of primary cross-link degradation due to photooxidation of transient ROH produced in reaction 5.

Conclusion

Curing and degradation chemistry in pigmented melamine formaldehyde cross-linked acrylic copolymer coat-

ings have been characterized as a function of depth at the primary cross-linking site by using the complementary techniques of diffuse reflectance infrared spectroscopy and solid-state ^{13}C NMR. The curing of an acid-catalyzed coating is shown to go to completion with respect to acrylic hydroxyl under the conditions used, with no significant concurrent melamine self-condensation reactions. Degradation is promoted by the presence of heat and/or light, residual acid, and atmospheric water; the degradative pathway invokes irreversible acid-catalyzed hydrolysis of residual $>NCH_2OCH_3$ throughout the coating and primary cross-links only at the very surface.

Acknowledgment. We gratefully acknowledge the skilled technical assistance of Dr. R. D. Farlee and Mr. R. H. Kern.

Registry No. CBT, 3071-66-7; methyl methacrylate–butyl acrylate–hydroxyethyl acrylate copolymer, 25951-38-6; *n*-propylamine, 107-10-8; cyanuric chloride, 108-77-0.

References and Notes

(1) D. R. Bauer and R. A. Dickie, *J. Polym. Sci., Polym. Phys. Ed.*, 18, 1997 (1980).
(2) D. R. Bauer and R. A. Dickie, *J. Polym. Sci., Polym. Phys. Ed.*, 18, 2015 (1980).
(3) W. J. Blank, *J. Coat. Technol.*, 51 (656), 61 (1979).
(4) D. R. Bauer, *J. Appl. Polym. Sci.*, 27, 3651 (1982).
(5) M. P. Fuller and P. R. Griffiths, *Anal. Chem.*, 50, 1906 (1978).
(6) R. H. Norton and R. J. Beer, *J. Opt. Soc. Am.*, 66, 259 (1976).
(7) E. O. Stejskal and J. Schaefer, *J. Magn. Reson.* 18, 560 (1975).
(8) J. W. Beams, *Rev. Sci. Instrum.*, 1, 667 (1930).
(9) E. R. Andrew, *Prog. NMR Spectrosc.*, 8, 1 (1972).
(10) A. C. Wang, A. N. Garroway, and W. M. Ritchey, *Macromolecules*, 14, 832 (1981).
(11) G. E. Meyers, *J. Appl. Polym. Sci.*, 26, 747 (1981).
(12) D. C. VanderHart, W. L. Earl, and A. N. Garroway, *J. Magn. Reson.*, 44, 361 (1981).
(13) J. S. Frye and G. E. Maciel, *J. Magn. Reson.*, 48, 125 (1982).
(14) A. Pines, M. G. Gibby, and J. S. Waugh, *J. Chem. Phys.*, 59, 569 (1973).
(15) D. E. Demco, J. Tegenfeldt, and J. S. Waugh, *Phys. Rev. B*, 11, 4133 (1975).
(16) M. Mehring, *NMR Basic Princ. Prog.*, 11, 112 (1976).
(17) W. T. Dixon, *J. Magn. Reson.*, 44, 220 (1981).
(18) W. T. Dixon, J. Schaefer, M. D. Sefcik, E. D. Stejskal, and R. A. McKay, *J. Magn. Reson.*, 45, 173 (1981).
(19) J. Herzfeld and A. E. Berger, *J. Chem. Phys.*, 73, 6021 (1980).
(20) A. D. English and R. D. Farlee, in progress.
(21) Reference 4 claims the identification of an infrared band at $\sim$1360 cm^{-1} that is thought to be characteristic of $>NCH_2N<$. We do not observe any spectroscopic changes in this region as a function of weathering or depth.
(22) Unpublished results.

Ordered Structure in Block Polymer Solutions. 3. Concentration Dependence of Microdomains in Nonselective Solvents

Mitsuhiro Shibayama, Takeji Hashimoto,* Hirokazu Hasegawa, and Hiromichi Kawai

Department of Polymer Chemistry, Faculty of Engineering, Kyoto University, Kyoto 606, Japan. *Received July 12, 1982*

ABSTRACT: Formation and development of the microdomain structure of a polystyrene–polyisoprene diblock polymer (SI) (having equal block molecular weights) in solutions with nonselective solvents were studied as a function of a wide range of polymer concentration (C) by means of the small-angle X-ray scattering (SAXS) technique with a position-sensitive detector and a high-power X-ray source. The lamellar microdomain with the identity period D starts to develop at concentration greater than 20 wt % polymer for the particular polymer–solvent pair. It was found that there are two regimes in the concentration dependence of D: (i) in the low-concentration regime (less than 70 wt % polymer in this system), which so far has not been studied by any researchers, D increases with increasing C, while (ii) in the high-concentration regime (greater than 70 wt % polymer), D tends to decrease with increasing C, consistent with earlier results reported by Skoulios et al. and Gallot et al. It is proposed that the increase of D with C in the low-concentration regime is due to increasing segregation power between polystyrene and polyisoprene in the presence of neutral solvent with increasing C and that the decrease of D with C in the high-concentration regime is due to a nonequilibrium effect; that is, the system cannot follow equilibrium appropriate for the higher concentrations within a given time scale of experiments. In this regime the average distance between the chemical junction points along the interface is virtually frozen in, and further removal of the solvent accompanied by increasing C simply results in shrinkage of the domain size perpendicular to the interface. The system can attain only "local" equilibrium and its minimum of free energy for a given fixed value of the average distance between the junction points.

I. Introduction

Existence of the ordered structure in block polymer solutions was first reported by Skoulios et al.[1-3] and later by Vanzo.[4] Further systematic but qualitative studies on the structure of the concentrated block polymer solutions have been carried out by French groups (Sadron, Gallot, Skoulios, and co-workers[5,6]) and also by a German group (Hoffmann and co-workers[7]). A good review was given by Gallot.[8]

These earlier studies were mostly concerned with the ordered structure of block polymers in selective solvents, especially with morphological transition of the microdomains (e.g., from spherical to cylindrical domains) and with change of the domain parameters with polymer concentration. In part 1 of this series, we discussed formation of spherical microdomains for a particular block polymer in a selective solvent and variations of its radius, intersphere distance (D_0), and long-range order over a wide range of volume concentration ϕ_p and temperature T.[9] At low ϕ_p, D_0 varies with $\phi_p^{-1/3}$, which can be described in terms of a deswelling effect, while at high ϕ_p, D_0 varies with $\phi_p^{-0.14}$. The low value of the exponent is due to increasing segregation power between the constituent block chains with increasing ϕ_p or to increasing repulsive interaction

0024-9297/83/2216-1427$01.50/0